Journal of Physics: Conference Series **770** (2016) 012032 doi:10.1088/1742-6596/770/1/012032

Search for Lepton Number Violation and resonances in the $K^{\pm} \to \pi\mu\mu$ at the NA48/2 experiment

C Lazzeroni on behalf of the NA48/2 Collaboration[1]

School of Physics and Astronomy, University of Birmingham, UK

E-mail: c.lazzeroni@bham.ac.uk

Abstract. Thanks to a large sample of kaon decays collected in 2003-2004, the NA48/2 experiment at CERN is able to set an upper limit on the rate of the lepton number violating decay $BR(K^{\pm} \to \pi^{\mp}\mu^{\pm}\mu^{\pm}) < 8.6 \times 10^{-11}$ at 90%CL, and to set limits at the $10^{-10} - 10^{-9}$ level on the appearance of resonances (including heavy neutral leptons N_4 and inflatons χ) in the $K^{\pm} \to \pi\mu\mu$ decays as functions of the resonance mass and lifetime.

1. Introduction

The observation of neutrino oscillations is so far the only indication of lepton flavour non-conversation; however models of physics beyond the Standard Model (SM) often include more general phenomena of Lepton Flavour Violation (LFV) and Lepton Number Violation (LNV). Besides, neutrino oscillations have demonstrated the massive nature of neutrinos; hence it is natural to include right-handed neutrino states in SM extensions. One of these extensions is the Neutrino Minimal Standard Model (νMSM)[1], in which three massive right-handed neutrinos are introduced to explain simultaneously neutrino oscillations, dark matter and baryon asymmetry of the Universe. The νMSM can be further extended by adding a real scalar field, to incorporate inflation and provide a common source for electroweak symmetry breaking and for right-handed neutrino masses[2]. These SM extensions predict new particles, such as heavy neutral leptons and inflatons, which could be produced in $K^{\pm} \to \pi\mu\mu$ decays: the Lepton Number Violating (LNV) $K^{\pm} \to \pi^{\mp}\mu^{\pm}\mu^{\pm}$ decay, forbidden in the SM, could instead proceed via the production of on-shell Majorana neutrinos, while inflatons χ could be produced in

[1] G. Anzivino, R. Arcidiacono, W. Baldini, S. Balev, J.R. Batley, M. Behler, S. Bifani, C. Biino, A. Bizzeti, B. Bloch-Devaux, G. Bocquet, N. Cabibbo, M. Calvetti, N. Cartiglia, A. Ceccucci, P. Cenci, C. Cerri, C. Cheshkov, J.B. Chèze, M. Clemencic, G. Collazuol, F. Costantini, A. Cotta Ramusino, D. Coward, D. Cundy, A. Dabrowski, P. Dalpiaz, C. Damiani, M. De Beer, J. Derré, H. Dibon, L. DiLella, N. Doble, K. Eppard, V. Falaleev, R. Fantechi, M. Fidecaro, L. Fiorini, M. Fiorini, T. Fonseca Martin, P.L. Frabetti, L. Gatignon, E. Gersabeck, A. Gianoli, S. Giudici, A. Gonidec, E. Goudzovski, S. Goy Lopez, M. Holder, P. Hristov, E. Iacopini, E. Imbergamo, M. Jeitler, G. Kalmus, V. Kekelidze, K. Kleinknecht, V. Kozhuharov, W. Kubischta, G. Lamanna, C. Lazzeroni, M. Lenti, L. Litov, D. Madigozhin, A. Maier, I. Mannelli, F. Marchetto, G. Marel, M. Markytan, P. Marouelli, M. Martini, L. Masetti, K. Massri, E. Mazzucato, A. Michetti, I. Mikulec, N. Molokanova, E. Monnier, U. Moosbrugger, C. Morales Morales, D.J. Munday, A. Nappi, G. Neuhofer, A. Norton, M. Patel, M. Pepe, A. Peters, F. Petrucci, M.C. Petrucci, B. Peyaud, M. Piccini, G. Pierazzini, I. Polenkevich, Yu. Potrebenikov, M. Raggi, B. Renk, P. Rubin, G. Ruggiero, M. Savrié, M. Scarpa, M. Shieh, M.W. Slater, M. Sozzi, S. Stoynev, E. Swallow, M. Szleper, M. Valdata-Nappi, B. Vallage, M. Velasco, M. Veltri, S. Venditti, M. Wache, H. Wahl, A. Walker, R. Wanke, L. Widhalm, A. Winhart, R. Winston, M.D. Wood, S.A. Wotton, A. Zinchenko, M. Ziolkowski.

$K^\pm \to \pi^\pm\chi$ decays, followed by $\chi \to \mu^+\mu^-$ [3]. In the following, the decays of interest $K^\pm \to \pi^\mp\mu^\pm\mu^\pm$ are denoted as KLNV and $K^\pm \to \pi^\pm\mu^+\mu^-$ are denoted as KLNC.

2. Experimental apparatus, data taking and selection of data samples

The NA48/2 experiment, located at the CERN SPS, was a multi-purpose experiment which collected data in 2003-2004, with simultaneous and collinear K^+ and K^- beams of the same momentum (60 ± 3.7) GeV/c produced by the 400 GeV/c SPS primary proton beam impinging on a Beryllium target. The kaon beams were steered into a 114 m long decay region, contained in a vacuum cylindrical tank sealed downstream by a convex Kevlar window; such window separated the vacuum from a magnetic spectrometer hosted in helium at atmospheric pressure. The spectrometer was formed of 4 drift chambers and a dipole magnet providing a horizontal momentum kick of 120 MeV/c. The spatial resolution of each chamber was $\sigma_x = \sigma_y = 90\mu$m, while the momentum resolution of the spectrometer was $\sigma(p)/p = (1.02 \oplus 0.044p)\%$, where the momentum p is measured in GeV/c. A hodoscope was placed downstream of the spectrometer and provided fast signals for trigger purposes, as well as time measurements for charged particles with a resolution of about 150 ps. The hodoscope was followed by a liquid Kripton electromagnetic calorimeter (LKr) electromagnetic calorimeter with a depth of 127 cm, corresponding to 27 radiation lengths. The LKr calorimeter energy resolution was $\sigma(E)/E = (3.2/\sqrt{E} \oplus 9.0/E \oplus 0.42)\%$, where E is the energy expressed in GeV. Downstream of the LKr, a muon detector consisted of three 2.7×2.7 m^2 planes of plastic scintillator strips, each preceded by a 80 cm thick iron wall and alternately aligned horizontally and vertically. The strips were 2.7 m long and 2 cm thick, and they were read out by photomultipliers at both ends. The widths of the strips were 25 cm in the first two planes, and 45 cm in the third plane. A detailed description of the NA48/2 beam line and the detector layout can be found in [4, 5].

The event selection for KLNV and KLNC decays and for resonance searches is based on the reconstruction of a three-track vertex, since the resolution of 50 cm on the vertex longitudinal position makes decays mediated by short-lived resonance particles (lifetime less than 10 ps) indistinguishable from a genuine three-track decay. The size of the selected $K \to \pi\mu\mu$ samples (denoted $K_{\pi\mu\mu}$ below) is normalised relative to the $K^\pm \to \pi^\pm\pi^+\pi^-$ decay channel (denoted $K_{3\pi}$ below). The advantage of this choice of normalisation channel is that both samples are collected concurrently using the same trigger logic; and that, given that the muon and pion masses are close, both final states have similar topologies leading to first order cancellation of the systematic effects induced by imperfect kaon beam description, local detector inefficiencies, and trigger inefficiency. There are no restrictions applied to additional energy depositions in the LKr calorimeter, or to extra tracks not belonging to the three-track vertex, to decrease the sensitivity to accidental activity.

The selections of both modes includes the requirement of a vertex satisfying the following criteria: total three-tracks charge = ± 1; vertex longitudinal position within the 98 m long fiducial decay volume; vertex tracks with momentum within the range (5;55) GeV/c; total momentum of the three track consistent with the beam nominal range (55;65) GeV/c; total transverse momentum of the three tracks with respect to the beam axis direction less than 0.010 GeV/c. If several vertices satisfy the above conditions, the one with the lowest fit χ^2 is considered. The vertex tracks are required to be consistent in time and to be in the detector geometric acceptances. Track separations are required to exceed 2 cm in the first chamber plane to suppress photon conversions, and 20 cm in the LKr and muon detector front planes to minimise particle misidentification due to shower overlaps and to multiple Coulomb scattering.

In order to select specifically the KLNV (KLNC) candidates, a vertex composed of one $\pi^\pm$ candidate and a pair of identically (oppositely) charged muon candidates is required, with the following additional criteria: for the pion, the ratio of energy E in the LKr calorimeter to momentum p measured in the spectrometer is $E/p < 0.95$ to suppress electrons; the pion

has no in-time associated hits in the muon detector; the muon candidates have $E/p < 0.2$ and associated hits in the first two planes of the muon detector; the pion candidate is required to have momentum above 15 GeV/c to ensure high muon rejection efficiency (in these conditions, the muon identification efficiency has been measured to be above 99% for $p > 15$ GeV/c). In addition the invariant mass of the three tracks in the $\pi^{\pm}\mu^{\pm}\mu^{\pm}$ ($\pi^{\pm}\mu^{+}\mu^{-}$) hypothesis must satisfy the requirement $|M_{\pi\mu\mu} - M_K| < 5$ MeV/c^2 ($|M_{\pi\mu\mu} - M_K| < 8$ MeV/c^2), where M_K is the nominal charged kaon mass, and the mass resolution is ± 2.5 MeV/c^2. An additional requirement is applied to the $K_{\pi\mu\mu}$ samples, when searching for resonances: the invariant mass M_{ij} of the ij pair ($ij = \pi^{\pm}\mu^{\mp}, \mu^{+}\mu^{-}$) must satisfy the condition $|M_{ij} - M_X| < 2\sigma(M_ij)$, where M_X is the assumed resonance mass and $\sigma(M_{ij})$ is the resolution on the invariant masses M_{ij}.

Independently, the following criteria are applied to select the $K_{3\pi}$ sample: pion identification criterion as above is applied to the odd-sign pion only, to symmetrize the selection of the signal and normalisation modes; the invariant mass of the three tracks is in the range $|M_{3\pi} - M_K| < 5$ MeV/c^2, corresponding to about ± 3 times its resolution. The number of charged kaon decays in the 98 m long fiducial decay region is computed as $N_K = N_{3\pi}D/Br(K_{3\pi})A(K_{3\pi}) = (1.64 \pm 0.01) \times 10^{11}$, where $N_{3\pi} = 1.37 \times 10^7$ is the number of data candidates reconstructed within the $K_{3\pi}$ selection, $D = 100$ is the downscaling factor, $BR(K_{3\pi})$ is the nominal branching ratio of the $K_{3\pi}$ decay mode, and $A(K_{3\pi}) = (14.955 \pm 0.004)\%$ is the acceptance of the $K_{3\pi}$ selection evaluated with MC simulations.

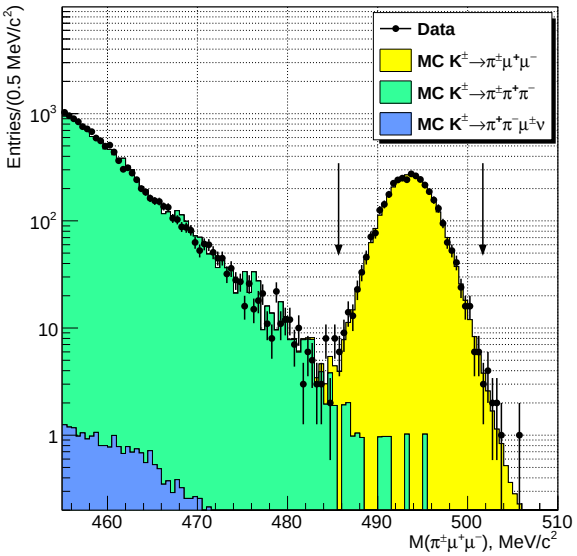

Figure 1. Invariant mass distribution of data and MC events for passing the KLNC selection.The signal mass region is indicated with vertical arrows.

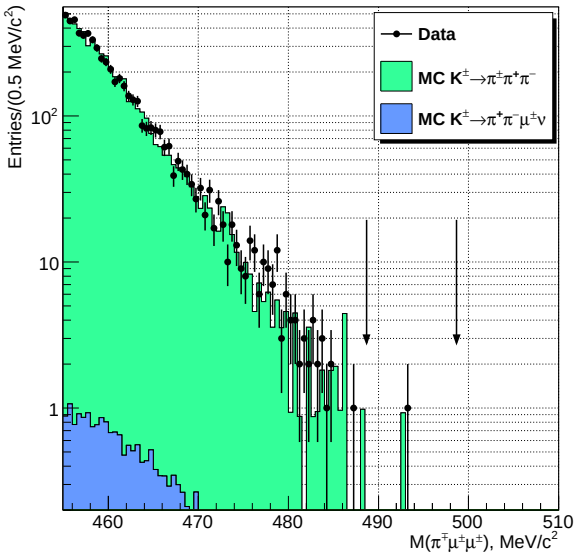

Figure 2. Invariant mass distribution of data and MC events for passing the KLNV selection.The signal mass region is indicated with vertical arrows.

3. Results

The statistical analysis to obtain the results shown here has been performed using a quasi-Newton minimisation algorithm to find numerically the 90% confidence intervals for the case of a Poisson process in presence of unknown backgrounds, by applying an extension of the Rolke-Lopez method [6].

The invariant mass distributions of data and MC events passing the KLNV and KLNC selections are shown in Fig. 1 and 2. One event is observed in the signal mass region (indicated

by vertical arrows) after applying the KLNV selection, while 3489 candidates are selected with the KLNC selection.

The main source of background in the KLNV sample is the $K_{3\pi}$ decay with two subsequent pion decays; the number of expected background events is $1.163 \pm 0.867_{stat} \pm 0.021_{ext} \pm 0.116_{syst}$. The corresponding upper limit at 90% CL on the number of $K^{\pm} \to \pi^{\mp}\mu^{\pm}\mu^{\pm}$ signal events in the KLNV sample is $N < 2.92$; using the values of the signal acceptance $(20.62 \pm 0.01)\%$ estimated with MC simulations and the number of kaon decays in the fiducial volume, this leads to a constraint on the signal branching ratio $BR(K^{\pm} \to \pi^{\mp}\mu^{\pm}\mu^{\pm}) < 8.6 \times 10^{-11}$ at 90% CL. The total systematic uncertainty on the quoted upper limit is 1.5%; the largest source is the limited accuracy of the MC simulations (1.0%), followed by uncertainties on the branching ratios of the normalisation and background channels.

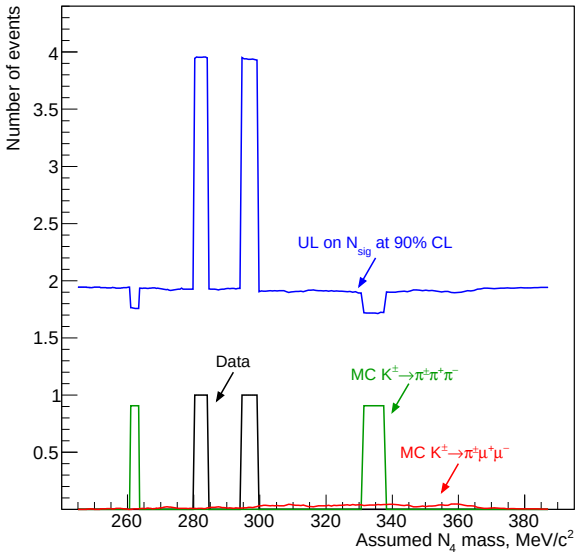

Figure 3. Numbers of observed data events (black) and expected background events ($K_{3\pi}$ in green, $K^{\pm} \to \pi^{\pm}\mu^{+}\mu^{-}$ in red) passing the $M_{\pi\mu}$ cut with the KLNV selection. The obtained upper limits at 90% CL on the numbers of signal candidates are shown for each resonance mass value (light blue).

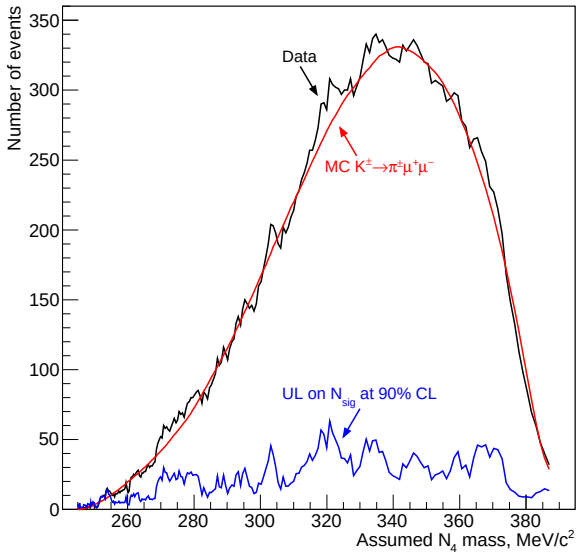

Figure 4. Numbers of observed data events (black) and expected background events ($K^{\pm} \to \pi^{\pm}\mu^{+}\mu^{-}$ in red) passing the $M_{\pi\mu}$ cut with the KLNC selection. The obtained upper limits at 90% CL on the numbers of signal candidates are shown for each resonance mass value (light blue).

The estimated $K_{3\pi}$ background contamination in the KLNC sample is $(0.36 \pm 0.10)\%$, based on MC simulations; this allows to consider the KLNC decay as the only background for the resonance searches in the collected KLNC sample. The acceptances for $K^{\pm} \to \mu^{\pm}X$ ($K^{\pm} \to \pi^{\pm}X$) decays with the subsequent $X \to \pi^{\pm}\mu^{\mp}$ ($X \to \mu^{+}\mu^{-}$) decay as a function of the resonance mass and lifetime has been evaluated with dedicated MC simulations; due to the required three-track topology of the selected events, the acceptances scale as $1/\tau$ for resonance lifetimes $\tau > 1$ ns. A peak search assuming different mass hypotheses has been performed over the distributions of the invariant masses M_{ij} (as defined above) of the selected $K_{\pi\mu\mu}$ samples. The mass steps of the resonance search is taken to be equal to $\sigma(M_{ij})/2$ and the half-width of the signal mass windows around the assumed mass is $2\sigma(M_{ij})$, where $\sigma(M_{ij})$ is the resolution on the invariant masses M_{ij}. It is worth mentioning that, as a consequence, the results obtained in the neighbouring mass hypotheses are highly correlated, since the signal mass window is about 8 times wider than the mass step of the resonance scan. In total, 284 (267) and 280 mass

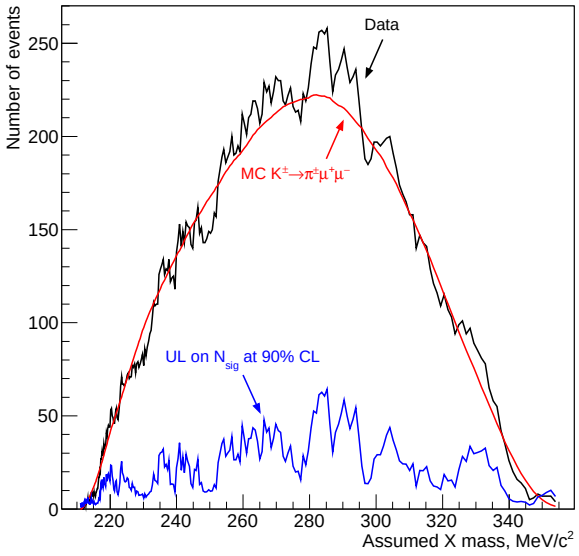

Figure 5. Numbers of observed data events (black) and expected background events ($K^{\pm} \to \pi^{\pm}\mu^{+}\mu^{-}$ in red) passing the $M_{\mu\mu}$ cut with the KLNC selection. The obtained upper limits at 90% CL on the numbers of signal candidates are shown for each resonance mass value (light blue).

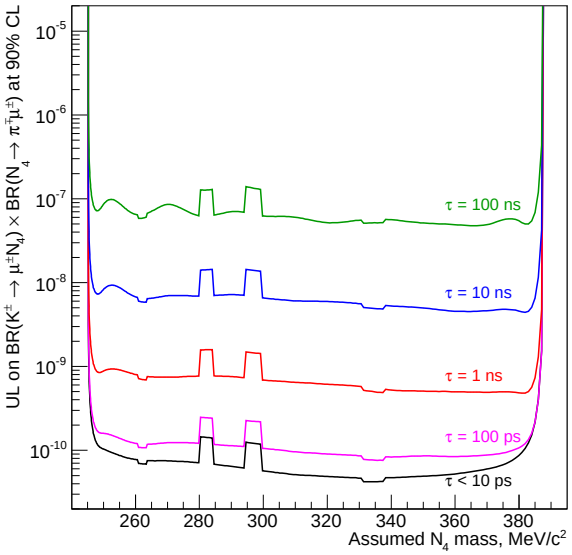

Figure 6. Obtained upper limits at 90% CL on the products of branching ratios as functions of the resonance mass and lifetime for $Br(K^{\pm} \to \mu^{\pm}N_4)Br(N_4 \to \pi^{\mp}\mu^{\pm})$.

hypotheses have been tested in the search of resonances in the $M_{\pi\mu}$ distribution of the KLNV (KLNC) candidates and in the $M_{\mu\mu}$ distribution of the KLNC candidates respectively. Here the statistical analysis has been performed in each mass window. The values of the observed data events in the signal mass window; the number of MC background events observed in the signal mass window and normalised to the size, with respect to the data volume, of the MC sample used to evaluate it; and the upper limit at 90% confidence level on the number of signal events obtained are shown for each mass hypothesis of the resonance searches in Fig. 3, 4, 5. For each of the three resonance searches performed, the local significance z of the signal has been evaluated for each mass hypothesis as $z = (N_{obs} - N_{exp})/\sqrt{(\delta N_{obs}^2 + \delta N_{exp}^2)}$, where N_{obs} is the number of observed events, N_{exp} is the number of expected background events, and δN_{obs} and δN_{exp} is the statistical uncertainty of N_{obs} and N_{exp} respectively. No signal is observed, as the local significances never exceed 3 standard deviations.

In absence of a signal, upper limits on the product $BR(K^{\pm} \to p_1X)BR(X \to p_2p_3)$ $(p_1p_2p_3 = \mu^{\pm}\pi^{\mp}\mu^{\pm}, \mu^{\pm}\pi^{\pm}\mu^{\mp}, \pi^{\pm}\mu^{+}\mu^{-})$ as a function of the resonance lifetime are obtained for each mass hypothesis, by using the values of the acceptances and the upper limits on the number of signal events for such mass hypothesis; the upper limits as a function of the resonance mass, for several values of the resonance lifetime, are shown in Fig. 6, 7, 8 .

4. Conclusions

The NA48/2 experiment at CERN has established an upper limit of 8.6×10^{-11} for the branching ratio of the Lepton Number Violating $K^{\pm} \to \pi^{\mp}\mu^{\pm}\mu^{\pm}$ decay, improving the best previous limit [7] by more than one order of magnitude. In addition, upper limits have been derived on the products of branching ratios $BR(K^{\pm} \to \mu^{\pm}N_4)BR(N_4 \to \pi\mu)$ and $BR(K^{\pm} \to \pi^{\pm}\chi)BR(\chi \to \mu^{+}\mu^{-})$ as functions of the resonance mass and lifetime; such limits

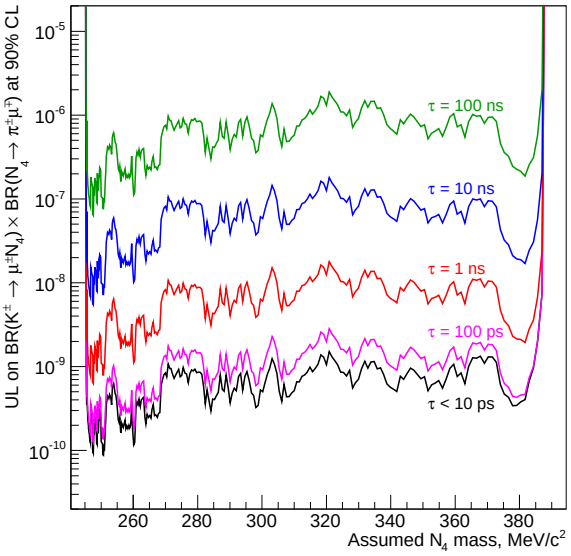

Figure 7. Obtained upper limits at 90% CL on the products of branching ratios as functions of the resonance mass and lifetime for $Br(K^{\pm} \to \mu^{\pm} N_4) Br(N_4 \to \pi^{\pm} \mu^{\mp})$.

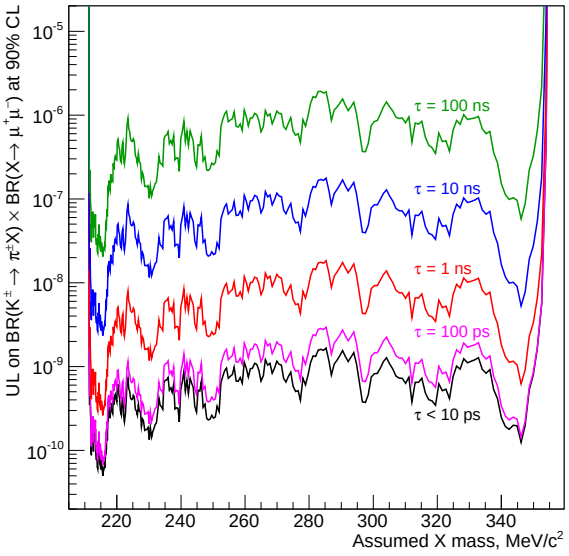

Figure 8. Obtained upper limits at 90% CL on the products of branching ratios as functions of the resonance mass and lifetime for $Br(K^{\pm} \to \pi^{\pm} \chi) Br(\chi \to \mu^{+} \mu^{-})$.

are in the $10^{-10} - 10^{-9}$ range for resonance lifetimes below 100 ps.

References

[1] T. Asaka and M. Shaposhnikov, Phys. Lett. B 620, 17 (2005).
[2] M. Shaposhnikov and I. Tkachev, Phys. Lett. B 639, 414 (2006).
[3] F. Bezrukov and D. Gorbunov, Phys. Lett. B 736, 494 (2014).
[4] J.R. Batley et al. (NA48/2 collaboration), Eur. Phys. J. C 52, 875 (2007).
[5] V. Fanti et al. (NA48 collaboration), Nucl. Instrum. Methods A 574, 433 (2007).
[6] W.A. Rolke and A.M. Lopez, Nucl. Instrum. Methods A 458, 745 (2001).
[7] J.R. Batley et al. (NA48/2 collaboration), Phys. Lett. B 697, 107 (2011).